3-2011

Use of 2nd and 3rd level correlation analysis for studying degradation in polycrystalline thin-film solar cells

David S. Albin
National Renewable Energy Laboratory

Joseph A. del Cueto
National Renewable Energy Laboratory

S. H. Demtsu
Primestar Solar

S. Bansal
GE Global Research Center

NREL
NATIONAL RENEWABLE ENERGY LABORATORY

The Use of 2nd and 3rd Level Correlation Analysis for Studying Degradation in Polycrystalline Thin-Film Solar Cells

D.S. Albin and J.A. del Cueto
National Renewable Energy Laboratory

S.H. Demtsu
Primestar Solar

S. Bansal
GE Global Research Center

Presented at the 35th IEEE Photovoltaic Specialists Conference (PVSC '10)
Honolulu, Hawaii
June 20-25, 2010

Conference Paper
NREL/CP-5200-48393
March 2011

Contract No. DE-AC36-08GO28308

NOTICE

Available electronically at http://www.osti.gov/bridge

Available for a processing fee to U.S. Department of Energy
and its contractors, in paper, from:

U.S. Department of Energy
Office of Scientific and Technical Information

P.O. Box 62
Oak Ridge, TN 37831-0062
phone: 865.576.8401
fax: 865.576.5728
email: mailto:reports@adonis.osti.gov

Available for sale to the public, in paper, from:

U.S. Department of Commerce
National Technical Information Service
5285 Port Royal Road
Springfield, VA 22161
phone: 800.553.6847
fax: 703.605.6900
email: orders@ntis.fedworld.gov
online ordering: http://www.ntis.gov/help/ordermethods.aspx

Cover Photos: (left to right) PIX 16416, PIX 17423, PIX 16560, PIX 17613, PIX 17436, PIX 17721

Printed on paper containing at least 50% wastepaper, including 10% post consumer waste.

THE USE OF 2ND AND 3RD LEVEL CORRELATION ANALYSIS FOR STUDYING DEGRADATION IN POLYCRYSTALLINE THIN-FILM SOLAR CELLS

D. S. Albin[1], J. A. del Cueto[1], S. H. Demtsu[2], and S. Bansal[3]
[1]National Renewable Energy Laboratory (NREL), Golden, CO USA
[2]Primestar Solar, Arvada, CO USA
[3]GE Global Research Center, Niskayuna, NY USA

ABSTRACT

The correlation of stress-induced changes in the performance of laboratory-made CdTe solar cells with various 2nd and 3rd level metrics is discussed. The overall behavior of aggregated data showing how cell efficiency changes as a function of open-circuit voltage (V_{oc}), short-circuit current density (J_{sc}), and fill factor (FF) is explained using a two-diode, PSpice model in which degradation is simulated by systematically changing model parameters. FF shows the highest correlation with performance during stress, and is subsequently shown to be most affected by shunt resistance, recombination and in some cases voltage-dependent collection. Large decreases in J_{sc} as well as increasing rates of V_{oc} degradation are related to voltage-dependent collection effects and catastrophic shunting respectively. Large decreases in V_{oc} in the absence of catastrophic shunting are attributed to increased recombination. The relevance of capacitance-derived data correlated with both V_{oc} and FF is discussed.

INTRODUCTION

Polycrystalline CdS/CdTe thin-film solar cells have demonstrated small-area, laboratory efficiencies of 16.5% [1]. The highest published efficiency for CdTe modules is 11.1% [2]. In addition to considerable research addressing efficiency, recent work has focused on understanding the durability of these thin-film semiconductor devices. The effects of back contact and processes on cell durability have been discussed for example in [3-5]. More recently, the detrimental effects of localized shunts [6], the general effects of film micro-nonuniformities [7], and the effect of cell-fabrication processing through formal design-of-experiments methodologies [8] have been reported.

The basic structure of a thin-film CdS/CdTe solar cell is that of a glass superstrate design in which light passes through a conducting/insulating (buffer) oxide film layer stack deposited on glass. Tin oxide (SnO_2) is the most common transparent conducting oxide (TCO), though there is considerable interest in the stannate compounds (Cd_2SnO_4 and $SnZnO_x$) for their superior optical properties [1].

Once transmitted through the glass/TCO/buffer superstrate, light is absorbed in the n-CdS/p-CdTe heterojunction structure, which provides the field necessary for charge separation. A back contact structure completes the cell. A schematic of this basic design is shown in Fig. 1.

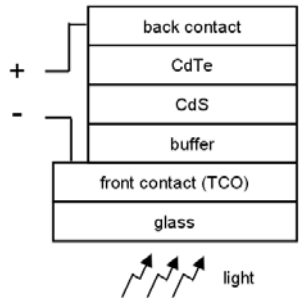

Figure 1 Basic CdS/CdTe solar cell design.

To ascertain durability, cells were fabricated and then exposed to 1-sun illumination under open-circuit, V_{oc}, bias and acceleration temperatures of 60 – 120 ºC for times exceeding 1000 hours [9]. Two dominant degradation mechanisms were identified in the temperature range studied. As shown in Fig. 2(a), from 60-80 ºC, an activation energy of 2.94 eV was measured and was attributed to S-outdiffusion from the CdS layer into the CdTe based on a reported value of 2.8 eV for bulk diffusion of S in CdTe [10]. This assertion was also supported by the observation of Kirkendall voids in the CdS layer. In the temperature range 100-120 ºC, an activation energy of 0.63 eV was determined, in good agreement with the reported value of 0.67 eV for Cu diffusion in CdTe [11].

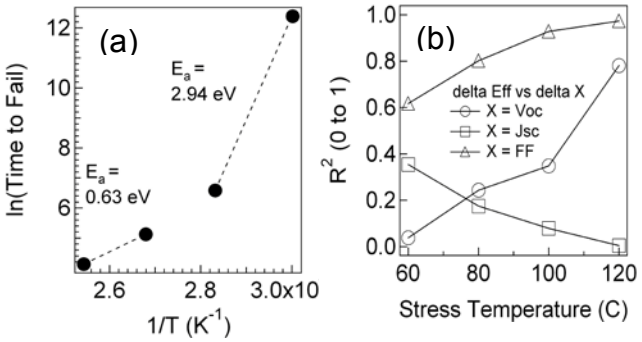

Figure 2 Degradation activation energies (a) and how the linear correlation (R^2) of Δη% changes with V_{oc}, J_{sc}, and FF as a function of stress temperature (b).

Since cell efficiency, η%, is determined by the equation:

$$\eta\% = V_{oc} \times J_{sc} \times FF \Big/ \phi_{inc}$$

(where Φ_{inc}, the incident power density, is typically normalized to a solar value of 100 mW/cm^2), a comparison of the linear correlation coefficients of $\Delta\eta\%$ versus changes in V_{oc}, short-circuit current density, J_{sc}, and fill factor, FF, during stress testing as a function of stress temperature was performed. This analysis is shown in Fig. 2(b). The moderate correlation of η% with J_{sc} seen at lower stress temperatures is due to reduced optical attenuation associated with S-outdiffusion from the CdS. The most important variable affecting η% at all temperatures, approaching an ideal value at 120 ºC, was FF.

Similar trends are observed when looking at aggregate cell stress data. Figure 3 is a plot of the percent change in efficiency (del Eff) vs. changes in V_{oc}, J_{sc}, and FF (del V_{oc}, del J_{sc}, and del FF, respectively) obtained in a set of 2052 measurements performed on CdTe devices stress tested at NREL with no regard to subtle changes in processing or stress conditions.

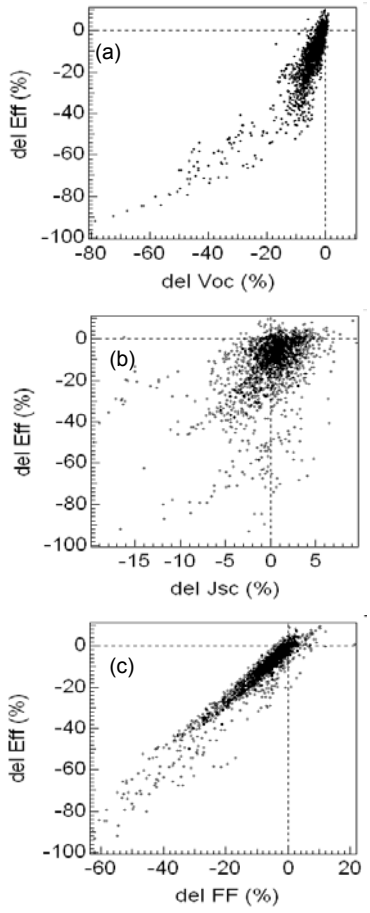

Figure 3 del Eff vs. del V_{oc}, J_{sc}, and FF.

The strong correlation of decreasing η% with both V_{oc} and FF is obvious, as is the general lack of correlation with J_{sc}. These figures also show possible annealing effects resulting in improved performance through increasing FF as well as the general observation that J_{sc} often increases during stress testing.

In this paper, through a combination of modelling and the examination of past data, we hope to provide a better understanding of why these correlations are observed between performance and changes in V_{oc}, J_{sc}, and FF.

J-V Curve Modeling

PSpice modeling provides an easy method by which to understand basic solar cell behavior. In Fig. 4, a parallel combination of forward-biased diodes is used to independently simulate recombination currents in the quasi neutral (J_{QNR}) and space charge (J_{SCR}). The back contact behavior is represented by the parallel combination of a reverse-biased diode (J_b) and shunt conductance ($1/R_b$) that was previously used to model performance characteristics observed in the first quadrant [12]. The theoretical basis for the two-diode model as a general expression for the current produced in a solar cell can be found in Ref. [13].

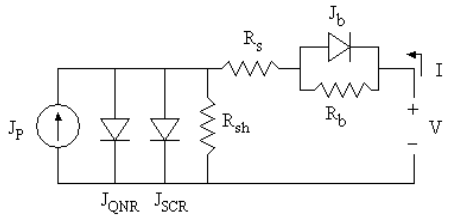

Figure 4 Two-diode solar cell discrete circuit model.

When the barrier height, E_b, associated with the back contact is low (E_b < 0.5 eV, J_b >100 mA/cm^2), the back contact impact on 4th quadrant behaviour, is minimized [12] such that the current-density, J, and voltage, V, of the solar cell is represented by:

$$J = J_{SCR} + J_{QNR} + \left(\frac{V - JR_s}{R_{sh}}\right) - J_{ph} \qquad (2)$$

where J_{SCR}, J_{QNR}, and J_{ph} are the recombination currents and photo generated current respectively, while R_s and R_{sh} represent series and parallel (shunt) resistance losses. J_{SCR} and J_{QNR} are further represented by the following:

$$J_{QNR} = J_{01}\left(e^{q(V-JR_s)/kT} - 1\right) \qquad (3)$$

$$J_{SCR} = J_{02}\left(e^{q(V-JR_s)/2kT} - 1\right) \qquad (4)$$

where J_{01} and J_{02} are further dependent upon minority carrier transport properties.

In the fourth quadrant, maximum power output is achieved by maximizing the term, J_{ph}, and minimizing the first three terms in (2), often referred to collectively as the "forward" current. Each of the forward current terms contributes to decreased cell performance. It should be noted that the recombination currents, J_{QNR}, and J_{SCR} are themselves dependent on resistive effects as shown in (3) and (4).

Using the J-V curve measured for a 14.4% cell fabricated at NREL, the percent that each parameter contributes to the forward current (and thus loss) in the power quadrant was determined and is shown in Fig. 5. This calculation used a fit-determined value of 3 Ω·cm^2 for R_s which is a reasonable upper value observed during stress testing of these cells [9].

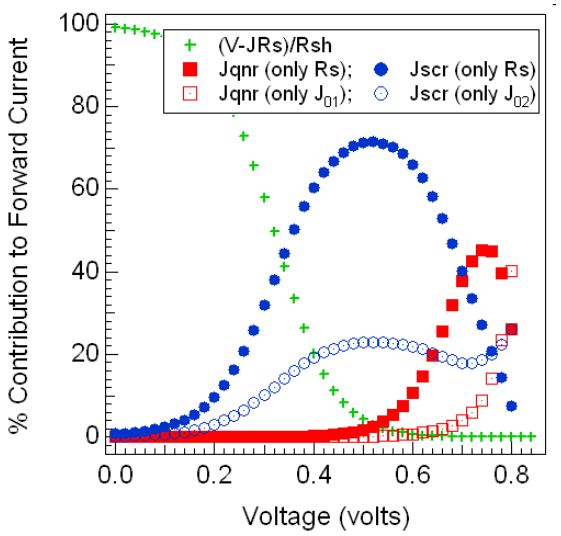

Figure 5 Forward current contributions to loss.

As seen in this figure, recombination occurs mostly in the space charge near V_{oc} where recombination in the quasi neutral region, i.e., between the depletion width and back contact, begins to dominate. Note that resistive contributions for both effectively go to zero at V_{oc} where J = 0 in equations (3) and (4). The voltage, V, at which J_{QNR} exceeds J_{SCR}, is given by the relation:

$$V = \frac{2kT}{q}\ln\left(J_{02}/J_{01}\right) \quad (5)$$

In *high* efficiency cells (smaller J_{02}) with higher V_{oc} values, the J_{01} term has a strong effect on V_{oc}. It is primarily for this reason that a two-diode model is preferred over one-diode models in which an "average diode factor (typically between 1 and 2) is usually determined. In general, if V_{oc} is less than 800 mV, the importance of J_{01} is reduced.

RESULTS AND DISCUSSION

Cell degradation during stress can be modeled by changing the discrete elements of Fig. 4. Increased recombination (J_{01}, J_{02}), resistive losses (increasing R_s, decreasing R_{sh}), and degraded backcontacts (decreasing J_b due to an increase in E_b, increased R_b) all cause performance to decrease. These effects on both the J-V characteristics of cells, and performance correlations similar to those shown in Fig. 3 were determined using PSpice as a modeling tool. For the sake of brevity, only important results explaining the behavior shown in Fig. 3 will be presented. An initial "baseline" cell with J_{01}=3e^{-16} A/cm^2, J_{02}=1e^{-09} A/cm^2, R_{sh} = 200 KΩ·cm^2, and R_s = 3 Ω·cm^2 was used as the point from which degradation in V_{oc}, J_{sc}, FF, and η% were determined.

Back contact degradation

A commonly observed degradation characteristic of CdTe solar cells is the formation of "roll-over" in the 1st quadrant. As mentioned previously, this effect can be modeled through introducing a contact diode leakage current, J_b which is inversely related to the back contact barrier height E_b [12]. Graphically, J_b can be estimated as the current at which the J-V curve "rolls over" in the 1st quadrant. For our simulations, a "baseline" value of E_b = 0.56 eV (which equates to J_b~10 mA/cm^2) and a value of R_b = 0. When R_b=0, the barrier is effectively absent in the 1st quadrant however it's appearance with degradation (as well as with low-temperature J-V measurements) confirms it's presence. Simulations were performed with E_b increasing to 0.68 eV (J_b~0.1 mA/cm^2) and R_b increasing as high as 100 Ω·cm^2.

The correlation of del Eff vs. del V_{oc}, del J_{sc}, and del FF assuming a nominal setting of R_b equal to 5 Ω·cm^2 is shown in Figure 6.

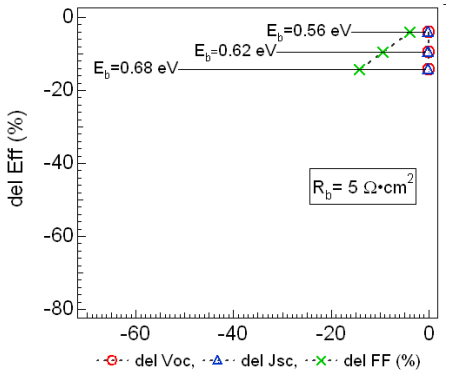

Figure 6 Efficiency change with contact barrier increase.

Figure 6 (and subsequent figures) has been scaled to allow comparison with Fig. 3. As seen in Fig. 6, a change in the back contact diode behavior only affects efficiency through FF. As the contact degrades, it affects neither V_{oc} nor J_{sc}. The increase in E_b shown in Fig. 5 is a worse-

case estimate as 1st quadrant behavior typically does not show such roll-over. The decrease in η% shown in Fig. 6 is thus not large enough to explain the η% vs. FF behavior shown in Fig. 3(c).

Resistive effects (R_{sh}, R_s)

Decreasing shunt resistance, R_{sh}, is a strong root cause for the behavior shown in Fig. 3(c). R_{sh} begins to affect FF as it approaches ~ 1000 Ω·cm^2, and V_{oc} and J_{sc} at a level closer to 100 Ω·cm^2. The correlation of del Eff vs. del V_{oc}, del J_{sc}, and del FF as R_{sh} decreases is shown in Figure 7.

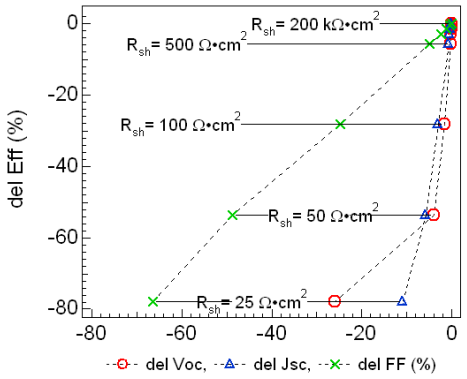

Figure 7 Efficiency change with decreasing R_{sh}.

Values of R_{sh} as low as 50-100 Ω·cm^2 can be observed during cell stress testing and can account for the large performance drops observed in Fig. 3. In cases of extreme shunting, J_{sc} can degrade by as much as 10%. The sharp increase in V_{oc} degradation occurring in extreme shunting (what might be referred to as catastrophic degradation) is also reflected in Fig. 3(a) where the rate of V_{oc} drop begins to increase greatly at a decreased performance level of ~40%.

A similar plot of the effect of series resistance, R_s, is shown in Fig. 8.

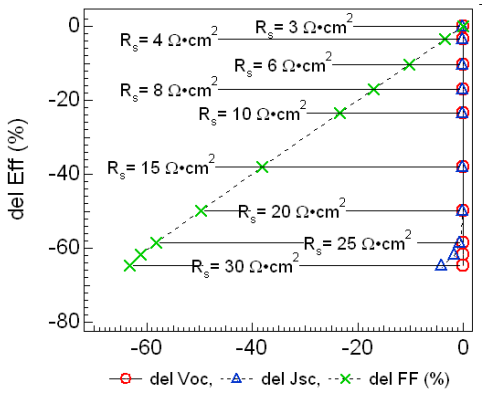

Figure 8 Efficiency change with increasing R_s.

Similar to R_{sh}, R_s can have a strong effect on FF, but differs in that it has no effect on V_{oc}, and only a very slight impact on J_{sc} at very high degradation levels. In practice, R_s is not observed to increase much from baseline levels and thus R_{sh} is believed to be more important in determining FF during stress testing.

Recombination

The effect of back contact and resistive degradation shown in Figs. 6, 7, and 8 do not adequately explain features observed in Fig. 3(a) and 3(b). Of these, only very large catastrophic decreases in R_{sh} (Fig. 7) can explain some of the large changes in V_{oc} and J_{sc} shown in Fig. 3. However, such changes are frequently observed in cells that do not exhibit "catastrophic" shunting.

Increased recombination was modeled by systematically increasing J_{02} from its baseline value of 1e^{-09} to 1e^{-06} A/cm^2. The corresponding correlation plot is shown in Fig. 9.

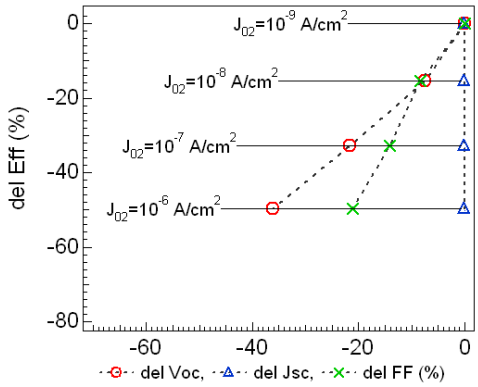

Figure 9 Efficiency change with increasing J_{02}.

An order magnitude increase in recombination current can account for most of the observed decrease in V_{oc} shown in Fig. 3(a) as well as a portion of the decrease in FF seen in Fig. 3(c). The fact that V_{oc} degrades during stress testing cells is a clear indicator of the importance in mitigating recombination in order to achieve stable cells.

As mentioned previously, significant decreases in J_{sc} have been observed where catastrophic shunting is not observed. Yet, the modeling performed with PSpice cannot explain this. The reason for this is due to the inability of PSpice to model a well-known effect in polycrystalline thin film cells known as voltage-dependent collection [14].

In PSpice simulations, this additional loss mechanism can be captured by properly adjusting the resistive model parameters. At V=0, the slope of the J-V curve can be used to accurately determine R_{sh}. The 1st quadrant behavior can then be used to adjust R_s in the absence of roll-over. If the latter is present, R_s can still be determined by fitting the curve between the maximum power point, P_{max} and V_{oc}. In doing so, voltage-dependent collection is

revealed as the difference between the model fit, and the actual J-V curve. Figure 8 is an example of this procedure applied to a cell where after 722 h of stress, η% had decreased 33% with a corresponding decrease in J_{sc} of 4.8%. In this example, neither R_{sh} (fixed by dV/dJ at V=0, or R_s (fixed by dV/dJ in the 1st quadrant) could adequately model the drop in J_{sc}. A comparison between the best model fit and the actual J-V curve is shown in Fig. 10.

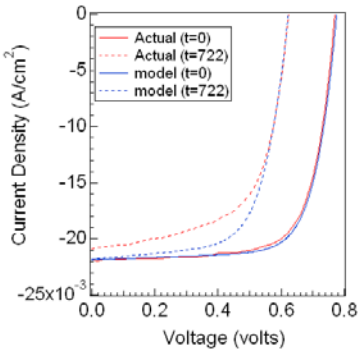

Figure 10 Voltage-dependent collection

The difference observed between the model-determined fit and the actual J-V curve after 722 h of stress (T = 125 ºC, V_{oc} bias, 1-sun illumination) is believed to reveal an additional voltage-dependent loss mechanism (not present at t=0) beyond recombination as represented by equations (3) and (4). No iteration of the discrete element parameters of the model shown in Fig. 4 can replicate the actual J-V curve. For the cell shown in Fig. 10, the additional voltage-dependent degradation introduced into the cell by stress testing corresponds to approximately a 0.96% and 3.78% increase in J_{sc} and FF loss, respectively.

3rd-Level Metric Correlations

The previous approach to understanding degradation requires little more than measuring and modeling details associated with J-V curves. In some measure, the incorporation of recombination terms provides a slight foray into more complex, higher-order parameters often extracted by sophisticated metrology tools and techniques. Unfortunately, the latter tools are often expensive and not readily available to those requiring many measurements in order to reach statistically viable conclusions. The techniques themselves often suffer from being too time-consuming or are entirely destructive or requiring ambient conditions that might introduce degradation not characteristic of field degradation in the cell. In order to increase our ability to probe for changes occurring in cells and modules during stress testing, we have recently developed and reported on the use of bi-directional voltage scans during capacitance measurements to both understand degradation [15] as well as to study and improve upon module stabilization procedures [16].

In Ref. [15], the relative durability of CdS/CdTe cells grown on either a bi-layer SnO_2 or cadmium/zinc stannate (CTO/ZTO) superstrate was evaluated. Cells grown on the latter typically exhibit greater V_{oc} and FF degradation than cells grown on the more common SnO_2-coated substrate. Using the two-direction, voltage scan method, capacitance-voltage (C-V) hysteresis in cells was determined as a function of stress time. Hysteresis is arbitrarily defined as the difference in W_d at V = 0 between reverse and forward direction scans, i.e., $W_{d,rev} - W_{d,fwd}$. Fig. 11 summarizes the variation of hysteresis with stress time as well as the correlation of both V_{oc} and FF with hysteresis determined in this study.

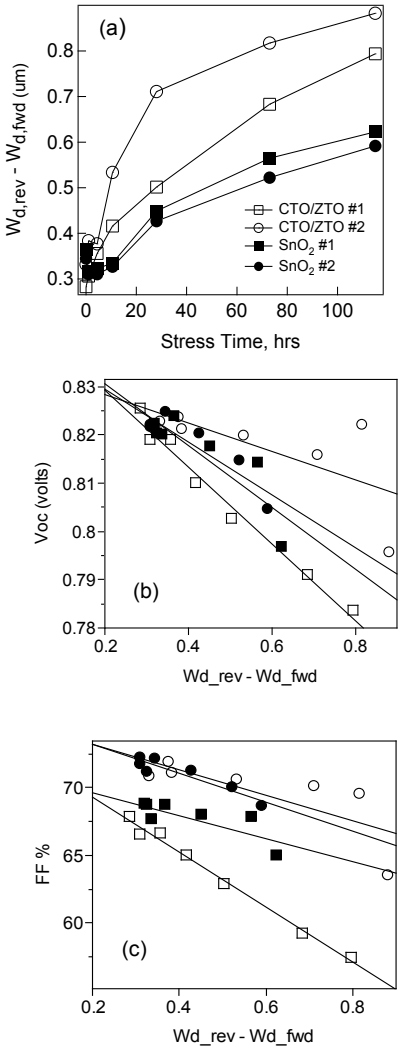

Figure 11 Variation of C-V hysteresis with stress time (a) for cells based on TCO-type and subsequent correlations of (b) V_{oc} and (c) FF with hysteresis.

The increased hysteresis shown in Fig. 11(a) was paralleled by a decrease in performance during stress. The correlation of hysteresis with both V_{oc} and FF (shown in Fig. 8(b) and 8(c), respectively) is also apparent. The correlation coefficient, R^2, of V_{oc} with hysteresis for

CTO/ZTO cells #1 and #2, and SnO_2 cells #1 and #2, were 0.98, 0.46, 0.75, and 0.82, respectively. The same values for FF were 0.99, 0.58, 0.63, and 0.87, respectively. Similar analysis performed without considering hysteresis, i.e., based on either $W_{d,fwd}$ or $W_{d,rev}$ separately were not nearly as high and tended to show non-monotonic behavior.

As discussed in Ref.[16], finished thin-film modules (including those based on $Cu(In,Ga)Se_2$) exhibit various degrees of hysteresis. The trends shown in Fig. 11 are in some cases replicated by the observations made on modules undergoing various tests to determine procedures to achieve stabilization prior to benchmarking performance. Figure 12 shows for example, the C-V hysteresis curves associated with two different completed CdTe modules after various conditioning exercises. More detail on the latter procedures can be found in Ref.[17].

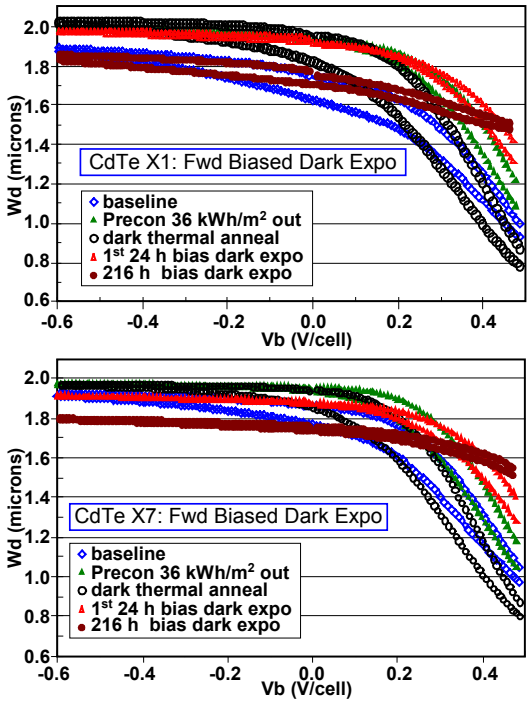

Figure 12 C-V hysteresis observed in finished production CdTe modules after various conditioning tests.

The greater hysteresis, and movement of the C-V determined W_d observed in module #X1 correlated with a performance degradation of ~8.3%. For module #X7, module performance decreased ~ 1.0% during test.

ACKNOWLEDGEMENT

The authors wish to thank our various industrial partners through whom we work collectively to understand and improve the fundamental durability of CdTe cells. We also acknowledge the support of the U.S. Department of Energy under Contract No. DOE-AC36-08G028308.

REFERENCES

[1] X. Wu, "High efficiency polycrystalline CdTe thin-film solar cells," Solar Energy 77, 2004, pp. 803-814.

[2] Publically available at www.firstsolar.com

[3] K. Dobson, I. Visoly-Fisher, G. Hodes, and D. Cahen, "Stabilizing CdTe/CdS Solar Cells with Cu-containing Contacts to p-CdTe," Advanced Materials, 13 (9), 2001, pp. 1495-1499.

[4] C. Corwine, A. Pudov, M. Gloeckler, S. Demtsu, and J. Sites, "Copper inclusion and migration from the back contact in CdTe solar cells, "Sol. Energy Mater. Sol. Cells, 82, 2004, pp. 481- 489.

[5] D. Albin, D. Levi, S. Asher, A. Balcioglu, "Precontact surface chemistry effects on CdS/CdTe solar cell performance and stability," Proc. 28th IEEE Photovoltaics Specialists Conference, New York, 2000, pp. 583-586.

[6] T. McMahon, T.J. Berniard, and D.S. Albin, "Nonlinear shunt paths in thin-film CdTe solar cells," J. Appl. Phys., 97, 2005, pg. 054503.

[7] V.G. Karpov, A.D. Compaan, and D. Shvydka, "Effects of nonuniformity in thin-film photovoltaics," Appl. Phys. Lett., 80 (22), 2005, pp. 4256-4258.

[8] D.S. Albin, S.H. Demtsu, and T.J. McMahon, "Film thickness and chemical processing effects on the stability of cadmium telluride solar cells," Thin Solid Films, 515, 2006, pp. 2659-2668.

[9] D.S. Albin, "Accelerated Stress Testing and Diagnostic Analysis of Degradation in CdTe Solar Cells," in Reliability of Photovoltaic Cells, Modules, Components, and Systems, edited by Neelkanth G. Dhere, Proceedings of SPIE Vol. 7048 (SPIE, Bellingham, WA, 2008) 70480N.

[10] B. McCandless, M. Engelmann, and R. Birkmire, "Interdiffusion of CdS/CdTe thin films: Modeling x-ray diffraction line profiles," J. Appl. Phys. 89(2), 2001, pp. 988-994.

[11] H. Woodbury and M. Aven, "Some Diffusion and Solubility Measurements of Cu in CdTe," J. Appl. Phys. 39(12), 1968, pp. 5485-5488.

[12] Demtsu, S., Sites, J., "Effect of back-contact barrier on thin-film CdTe solar cells," Thin Solid Films 510, 2006, pp. 320-324.

[13] Luque, A., Hegedus, S., eds., [Handbook of Photovoltaic Science and Engineering], John Wiley & Sons, in particular Gray, J., Chapter 3 "The Physics of the Solar Cell,", (2003).

[14] S.S. Hegedus and W.N. Shafarman, "Thin-Film Solar Cells: Device Measurements and Analysis," Prog. Photovolt: Res. Appl. 2004; 12:155-176.

[15] D.S. Albin, R.G. Dhere, S.C. Glynn, et al., "Degradation and capacitance-voltage hysteresis in CdTe Devices," Proceedings of SPIE Vol. 7412, 74120I (2009).

[16] del Cueto, J.A., Deline, C.A., Albin, D.S., et al., "Striving for a standard protocol for preconditioning or stabilization of polycrystalline thin film photovoltaic modules," Proceedings of SPIE Vol. 7412, 741204 (2009).

[17] del Cueto, J.A., Deline, C.S., Rummel, S.R., and Anderberg, A., “Progress Toward a Stabilization and Preconditioning Protocol for Polycrystalline Thin-Film Photovoltaic Modules”, [ibid].

REPORT DOCUMENTATION PAGE

Form Approved
OMB No. 0704-0188

PLEASE DO NOT RETURN YOUR FORM TO THE ABOVE ORGANIZATION.

1. REPORT DATE *(DD-MM-YYYY)*	2. REPORT TYPE	3. DATES COVERED *(From - To)*
March 2011	Conference Paper	

4. TITLE AND SUBTITLE
The Use of 2nd and 3rd Level Correlation Analysis for Studying Degradation in Polycrystalline Thin-Film Solar Cells

5a. CONTRACT NUMBER
DE-AC36-08GO28308

5b. GRANT NUMBER

5c. PROGRAM ELEMENT NUMBER

6. AUTHOR(S)
D.S. Albin, J.A. del Cueto, S.H. Demtsu, and S. Bansal

5d. PROJECT NUMBER
NREL/CP-5200-48393

5e. TASK NUMBER

5f. WORK UNIT NUMBER

7. PERFORMING ORGANIZATION NAME(S) AND ADDRESS(ES)
National Renewable Energy Laboratory
1617 Cole Blvd.
Golden, CO 80401-3393

8. PERFORMING ORGANIZATION REPORT NUMBER
NREL/CP-5200-48393

9. SPONSORING/MONITORING AGENCY NAME(S) AND ADDRESS(ES)

10. SPONSOR/MONITOR'S ACRONYM(S)
NREL

11. SPONSORING/MONITORING AGENCY REPORT NUMBER

12. DISTRIBUTION AVAILABILITY STATEMENT
National Technical Information Service
U.S. Department of Commerce
5285 Port Royal Road
Springfield, VA 22161

13. SUPPLEMENTARY NOTES

14. ABSTRACT *(Maximum 200 Words)*

The correlation of stress-induced changes in the performance of laboratory-made CdTe solar cells with various 2nd and 3rd level metrics is discussed. The overall behavior of aggregated data showing how cell efficiency changes as a function of open-circuit voltage (Voc), short-circuit current density (Jsc), and fill factor (FF) is explained using a two-diode, PSpice model in which degradation is simulated by systematically changing model parameters. FF shows the highest correlation with performance during stress, and is subsequently shown to be most affected by shunt resistance, recombination and in some cases voltage-dependent collection. Large decreases in Jsc as well as increasing rates of Voc degradation are related to voltage-dependent collection effects and catastrophic shunting respectively. Large decreases in Voc in the absence of catastrophic shunting are attributed to increased recombination. The relevance of capacitance-derived data correlated with both Voc and FF is discussed.

15. SUBJECT TERMS
CdTe solar cell; degradation; stress

16. SECURITY CLASSIFICATION OF:			17. LIMITATION OF ABSTRACT	18. NUMBER OF PAGES	19a. NAME OF RESPONSIBLE PERSON
a. REPORT	b. ABSTRACT	c. THIS PAGE			19b. TELEPHONE NUMBER (*Include area code*)
Unclassified	Unclassified	Unclassified	UL		